*IOSR Journal of Applied Chemistry (IOSR-JAC)*
*e-ISSN: 2278-5736.Volume 10, Issue 9 Ver. I (September. 2017), PP 31-44*
*www.iosrjournals.org*

# The photocatalytic degradation of Methyl Green in presence of Visible light with photoactive $Ni_{0.10}$:$La_{0.05}$:$TiO_2$ nanocomposites

Azad Kumar*, Gajanan Pandey
*Department of Applied Chemistry, School for physical Sciences,*
*Babasaheb Bhimrao Ambedkar University, Lucknow-226025, India*
*Corresponding author: Azad Kumar (kumarazad20@gmail.com)*

***Abstract:*** *In this paper, we have done the photodegradation of Methyl green dye in presence of prepared $Ni_{0.10}$:$La_{0.05}$:$TiO_2$ nanocomposites. The nanocomposites of $Ni_{0.10}$:$La_{0.05}$:$TiO_2$ was prepared by the solution impregnation method. The characterization of Synthesized $TiO_2$ and $Ni_{0.10}$:$La_{0.05}$:$TiO_2$ nanocomposites were done by X-Ray Diffractometer, SEM, TEM, UV- Vis, FT-IR, Band gap energy and BET. The photocatalytic degradation of Methyl Green has been done in presence of $TiO_2$ and $Ni_{0.10}$:$La_{0.05}$:$TiO_2$ nanocomposites. The presence of anatase and rutile phase in the nanocomposites has been confirmed by XRD analysis. The photocatalysts particle was found in nanodiamension in morphology. The surface area was observed 34.72 and 96.58 $m^2/g$ for the $TiO_2$ and $Ni_{0.10}$:$La_{0.05}$:$TiO_2$ nanocomposites. The band gap energy was observed 3.2 and 3.0 eV for the $TiO_2$ and $Ni_{0.10}$:$La_{0.05}$:$TiO_2$ nanocomposites. The photocatalytic degradation behaviour of photocatalysts was investigated by considering different parameters such as effect of concentration, effect of amount of photocatalyst, effect of pH, effect of temperature, adsorption and kinetics. The 90-98 % photodegradation of Methyl Green has been found at 7 pH, 25 ppm concentration of dye, 800 mg/L amount of photocatalyst and 50 min illumination of visible light in presence of $Ni_{0.10}$:$La_{0.05}$:$TiO_2$ while 10-18 % in presence of neat $TiO_2$ . The photodegradation of Methyl Green was following the first order kinetics.*

***Keyword:*** *Photodegradation, photocatalyst, photocatalysis, Methyl Green, nanocomposite.*

---

Date of Submission: 21-08-2017 Date of acceptance: 08-09-2017

---

## I. Introduction

Cationic triphenylmethane dyes have found extensive use as colorants in industry and as antimicrobial agents [1]. Recent reports indicate that they may further serve as targetable sensitizers in the photodestruction of specific cellular components or cells [2-3]. Methyl green (MG) is a basic triphenylmethane-type dicationic dye, usually used for staining solutions in medicine and biology and as a photochromophore to sensitize gelatinous films [4]. Cationic (basic) dyes have been used for paper, polyacrylonitrile, modified polyesters, polyethylene terephthalate, and, to some extent, in medicine. Originally they were used for silk, wool, and tannin-mordant cotton [5]. These water-soluble dyes yield colored cations in solution and that is why they are called cationic dyes. It has been used to differentiate between deoxyribonucleic acid and ribonucleic acid [6]. The binding of Methyl Green to DNA is probably ionic, as opposed to intercalative, and it remains so stably bound to double stranded DNA that, with its conversion to the colourless carbinol form, it has been used to assess the binding of other molecules to DNA [7-8]. However, great concern has arisen about the thyroid peroxidase-catalyzed oxidation of the triphenylmethane class of dyes because the reactions might form various N-de-alkylated primary and secondary aromatic amines, with structures similar to aromatic amine carcinogens [9].

Dyes are the most resistant compounds and used in various industries. The industrial effluents are causing adverse environmental problems [10-11]. Most of the dyes used in the pigmentation of textiles, leather, paper, ceramics, and food-processing are derived from azo dyes. Dyes are lost with waste water during synthesis and processing [12-13]. This represents a great hazard to human and environmental health due to the toxicity of azo dyes [14]. The treatment of such pollutants can be achieved by heterogeneous photocatalysis due to its efficiency and low cost as well as to the fact that it allows complete degradation of pollutants to carbon dioxide and inorganic acids [15-16].

Titanium dioxide $TiO_2$ is a most important nano material which has attracted a great attention due to its unique properties [17]. Titanium dioxide $TiO_2$ have excellent merits in solar energy transferring and photocatalysis of poison compounds in environment. The chemical inertness and the non-toxicity of $TiO_2$ have also made it a superior photocatalyst [18-19]. Titania has a large band gap (3.20 ev for anatase $TiO_2$) and therefore, only a small fraction of solar light can be absorbed [20-21]. Many attempts have been made to sensitize titanium dioxide to the whole visible region, such as impregnation with transition metals [22-23], transition metal ions [24], non-metal atoms [24] and organic materials [25]. Introduction of dopant allows

Titania to absorb in the visible region but this does not necessarily mean that the doped catalyst has a better photocatalytic activity [26].

In this study, to prepared the nanocomposites of $Ni_{0.10}$:$La_{0.05}$:$TiO_2$ by the solution impregnation method. Synthesized $TiO_2$ and $Ni_{0.10}$:$La_{0.05}$:$TiO_2$ were characterized by X-Ray Diffractometer, SEM, TEM, UV- Vis, FT-IR, Band gap energy and BET. The $TiO_2$ and $Ni_{0.10}$:$La_{0.05}$:$TiO_2$ were used as photocatalyst for the degradation of Methyl Green. We have investigated the photocatalytic degradation behaviour of cationic dye molecule from aqueous system onto prepared $Ni_{0.10}$:$La_{0.05}$:$TiO_2$ nanocomposites by taking methyl green as model molecule (showing in Figure 1). The photocatalytic degradation behaviour was investigated by considering different parameters such as effect of concentration, effect of amount of photocatalyst, effect of pH, effect of temperature, adsorption and kinetics.

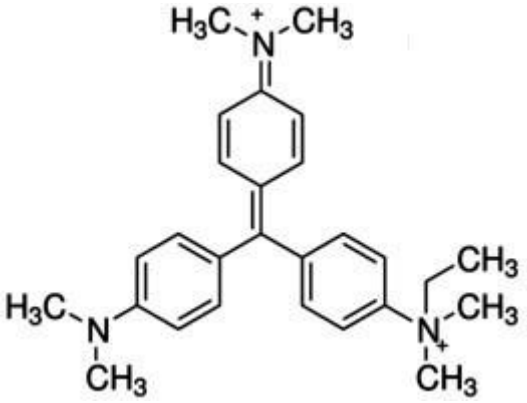

**Fig. 1** Structure of Methyl Green dye

## II. Methodology

### 2.1 Preparation of the photocatalysts

In this method, 10 ml of $TiCl_4$ solution (1000 mg/l), 2ml of 0.1M Nickel acetate, 1ml of 0.1M Lanthanum nitrate and NaOH solution (64.5 g/l) was added drop wise to water with stirring. After the resulting solution reaches pH to 7, the slurry was filtered, and the filter cake of $TiO_2$ was washed and redispersed in water to prepare 1 M of $TiO_2$ slurry. Resulting $TiO_2$ slurry and an aqueous solution of $HNO_3$ were refluxed at $95^0$C for 2 h, cooled to room temperature and neutralized with 28% of aqueous ammonia. Then, it was filtered, washed and calcined at 400 $^o$C. The $Ni_{0.10}$:$La_{0.05}$:$TiO_2$ nanocomposites were prepared by solution impregnation method. In this method suitable quantity of prepared $TiO_2$ (2 g) was dispersed in alcoholic Nickel acetate 10% (w/v) and lanthanum nitrate 5% (w/v). The dispersion is agitated continuously for 4 hour at 80 $^o$C temperature. After the treatment the residue was removed through filtration and was sintered for 4 hour in presence of air at 600 $^o$C by kipping it in a silica crucible inside the muffle furnace. After sintering and slow anilling to room temperature, content was taken out from furnace and was stored in air tight bottles and was used as photocatalyst [27-31].

$$TiCl_4 + 4NaOH \longrightarrow Ti(OH)_4 + 4NaCl \quad (1)$$

$$Ti(OH)_4 \longrightarrow TiO_2 + 2H_2O \quad (2)$$

$$TiO_2 + 10\ \%\ Ni(CH_3COOH)_3 + 5\ \%\ La(NO_3)_3 \longrightarrow Ni_{0.10}:La_{0\cdot05}:TiO_2 \quad (3)$$

### 2.2. Photocatalyst characterization

#### 2.1.1. Powder x-ray diffraction analysis (P-XRD)

The physical properties of metal oxide semiconductor nanocomposites that may influence significantly their use as photocatalyst are dependent on nature of crystalline phase present. Thus, phase analysis is an important parameter for this study and the prepared samples were subjected to x-ray diffraction analysis on Powder X-Ray Diffractometer (Bruker AXS D8 Advance System, Germany). The observed X-Ray diffractogram of samples were analyzed further to estimate average grain size in the sample by Scherrer's calculation [32].

$$T = \frac{0.9\,\lambda}{\beta\,\mathrm{Cos}\theta} \quad (4)$$

Where, T is the mean size of the ordered (crystalline) domains, which may be smaller or equal to the grain size, *K* is a dimensionless shape factor, with a value close to unity. The shape factor has a typical value of about 0.9, but varies with the actual shape of the crystallite, $\lambda$ is the X-ray wavelength, $\beta$ is the line broadening at half the maximum intensity (FWHM), after subtracting the instrumental line broadening, in radians. This quantity is also sometimes denoted as $\Delta(2\theta)$, $\theta$ is the Bragg angle.

**2.2.2. SEM analysis**

The particle morphologies of the photocatalyst were studied using scanning electron microscope. Samples were mounted on aluminum stab with the help of double-sided tape. Mounted stabs were coated with gold palladium prior to analysis using a Polaron sputter coater.

**2.2.3. TEM analysis**

The particle morphologies of the photocatalyst were studied by using Transmission electron microscopy (TEM, JEOL JEM 2011 equipped with LaB6 filament). The TEM images were collected with a 4008 - 2672 pixel CCD camera (Gatan Orius SC1000) coupled with the DIGITAL MICROGRAPH software. Coupled chemical analyses were obtained by an EDX micro- analyzer (PGT IMIX PC).

**2.2.4. BET surface area analyser**

The surface area and pore characteristics of the derived photocatalyst was determined from nitrogen adsorption/desorption isotherms at 77 K (boiling point of nitrogen gas at 1atm pressure) using a BET surface area analyzer (BELSORP-max, Japan).

**2.2.5. UV-Visible spectrophotometer**

Since the absorption of light by photocatalyst is the most crucial step in any photocatalysed reaction, and is decided primarily by the band gap energy of material, attempt would also be made to evaluate band gap energy employing a UV spectrometer (UV 2450 Shimadzu).

**2.2.6. Fourier transforms Infrared spectroscopy (FTIR)**

The Photocatalyst (2 mg) was mixed with 200 mg of KBr and then pelleted. The FT-IR spectra of the pellets were recorded using a Fourier Transform Infra-Red Spectrometer (FTIR) Thermo Scientific (Nicole 6700).

**2.3. Dark adsorption studies**

The adsorption studies were performed using aqueous solutions of EBT. For this purpose 20 ml dye solution of different concentrations (25-100 ppm) were magnetically stirred separately in presence of bare and metal impregnated catalysts (0.5g) in dark up to 30 min. Thereafter, the suspensions were collected after regular time intervals (5 min) filtered through cellulose filter and then sample were analyzed by UV-vis spectrophotometer at λmax = 631.5 nm for Methyl Green [33].

**2.4. Photo-degradation of dyes**

In this study by the photo-catalytic degradation of Methyl Green was investigated. A solution of dye in water: alcohol (10:1 V/V) was prepared and in this solution a suitable quantity of photocatalyst (100 to 800 mg/L) was dispersed. The dispersion was subjected to Visible light irradiation (500 W Tungsten Lamp were used for the visible light radiation in a close chamber) for varying duration and after desired irradiation the residual concentration of dye in the solution was determine spectrophotometrically by taken out suitable aliquot of dispersion and removal of photocatalyst by centrifugation. A quantitative estimation of dye concentration spectrometric observation when recorded only at the experimental determines λ max value which is 631.5 nm [34-43]. The % degradation efficiency of Methyl Green dye was calculated by Equation (5).

$$\eta\ \% = \frac{A_O - A_F}{A_O} * \mathbf{100} \qquad (5)$$

## III. Results

**3.1. Characterization of Photocatalyst**

**3.1.1. Phase identification by X-ray diffraction analysis**

The obtained X-Ray diffraction patterns of $TiO_2$ and $Ni_{0.10}$:$La_{0.05}$:$TiO_2$ are shown in Figures 2. The observed pattern of peaks, when compared with the standard JCPDS database, suggested that, in prepared $TiO_2$ sample, major peaks at 2θ = 25.5° 37.2, 48.3, and 54.4, which can be indexed to the (101), (004), (200), and (211) crystal facets of anatase $TiO_2$ (JCPDS File number: 21-1272). Whereas major peaks at 2θ = 26.9º and 28.2º indicate the presence of rutile phase which can indexed to the (110), (121), respectively [32]. In case of $Ni_{0.10}$:$La_{0.05}$:$TiO_2$ sample, the observed XRD pattern indicates not only a change in the peak intensity, compared to $TiO_2$, but even the absence of some originally observed $TiO_2$ peaks [44]. This is, probably, due to the change in the crystallinity and grain fragmentation, when the samples were wet impregnated by Nickel and Lanthanum. Utilizing the observed X-ray diffraction data of samples, Scherrer's calculations were attempted to know the average size of particles/grains in the samples [32]. Although, Scherrer's calculations are only approximate in nature, but definitely provide a first-hand idea of the average size of the crystal in the samples, which may be quite accurate, provided the size of crystal is below 100 nm.

The mean size of $TiO_2$ and $Ni_{0.10}$:$La_{0.05}$:$TiO_2$ nanocomposites, calculated by Scherrer's Equation, are about 76 and 34 nm respectively. The results of Scherrer's calculations are presented in Table 1. The results suggest average size of the crystal in the samples lying in nm range. The result is in good agreement with the TEM.

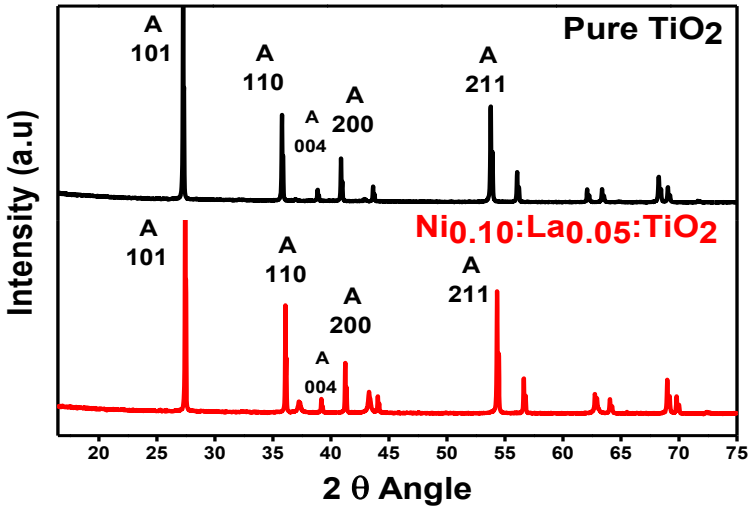


**Fig.2.** Observed XRD pattern $TiO_2$ and $Ni_{0.10}$:$La_{0.05}$:$TiO_2$

**Table 1:-** Average size of crystal in the samples of $TiO_2$ and $Ni_{0.10}$:$La_{0.05}$:$TiO_2$.

| Sample | Particle Size (nm) |
|---|---|
| $TiO_2$ | 76 |
| $Ni_{0.10}$:$La_{0.05}$:$TiO_2$ | 34 |

### 3.1.2. UV-Vis spectra

Aqueous suspensions of the samples were used for the UV absorption studies. The absorption spectrum of $TiO_2$ consists of a single broad intense absorption between 383 nm due to the charge-transfer from the valence band to the conduction band [45]. The undoped $TiO_2$ showed absorbance in the shorter wavelength region while $Ni_{0.10}$:$La_{0.05}$:$TiO_2$ result showed slight red shift in the absorption edge. The absorption peak of $Ni_{0.10}$:$La_{0.05}$:$TiO_2$ was found at 410 nm. It is showing in Figure 3. The impregnation of Ni and La ions into $TiO_2$ could shift optical absorption edge from UV to visible range, but slight change in $TiO_2$ band gap was observed [46-47].

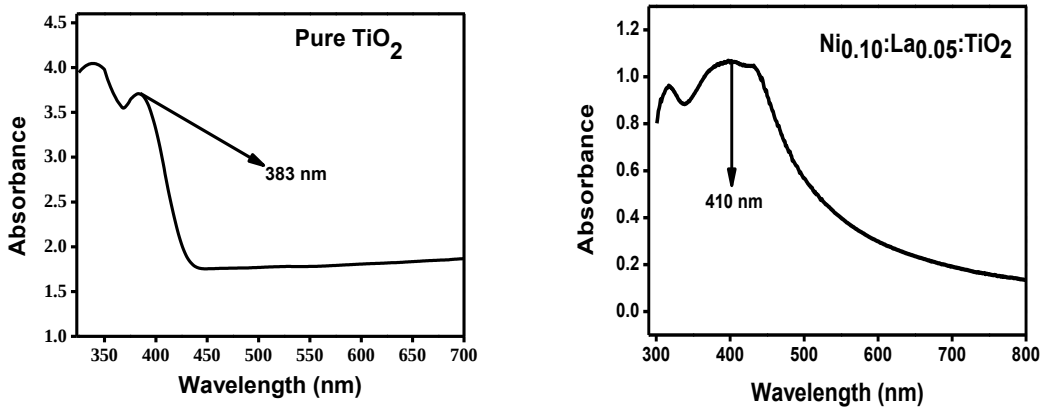


**Fig.3**. UV- spectra of $TiO_2$ and $Ni_{0.10}$:$La_{0.05}$:$TiO_2$

### 3.1.3. Band gap energy determination

The band gap of samples was calculated by extrapolation of the $(\alpha h\nu)^2$ versus $h\nu$ plots, where $\alpha$ is the absorption coefficient and $h\nu$ is the photon energy, $h\nu = (1239/\lambda)$ eV. The value of $h\nu$ extrapolated to $\alpha = 0$ gives an absorption energy, which corresponds to a band gap ($E$g). From the Figure 4 we found an $E$g value of 3.2 eV for $TiO_2$ and 3.0 for $Ni_{0.10}$:$La_{0.05}$:$TiO_2$ [48]. The slight decrease in band gap energy in case of $Ni_{0.10}$:$La_{0.05}$:$TiO_2$ is due to formation of sub-band level between valence band and conduction band caused impregnation of $Ni^{2+}$ and $La^{3+}$ ions in $TiO_2$ host [49].

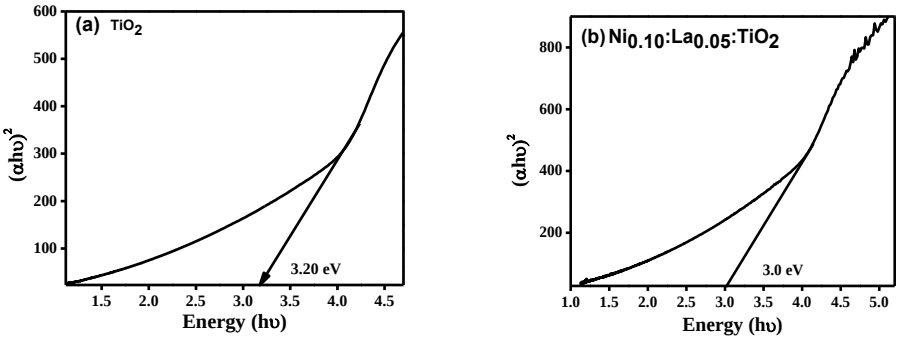


**Fig.4.** Band gap energy of (a) $TiO_2$ (b) $Ni_{0.10}$:$La_{0.05}$:$TiO_2$

### 3.1.4. FT-IR spectroscopy

FT-IR spectra of undoped and 10% Ni and 5% La impregnated $TiO_2$ samples (Figure 5) show peaks corresponding to stretching vibrations of the O-H and bending vibrations of the adsorbed water molecules around 3350-3450 $cm^{-1}$ and 1620-1635 $cm^{-1}$, respectively. The broad intense band below 820, 804, 592 and 456 $cm^{-1}$ is due to Ti-O-Ti vibrations. The shift to the higher wave numbers and sharpening of the Ti-O-Ti band may be due to decrease in size of the catalyst nanoparticles. In addition, the surface hydroxyl groups in $TiO_2$ increased with the increasing of Ni loading, which is confirmed by increase in intensity of the corresponding peaks. The FT-IR spectra of $Ni_{0.10}$:$La_{0.05}$:$TiO_2$ show strong band at 1075 $cm^{-1}$, corresponds to the vibration of Ni–O bond and confirms the penetration of nickel in Titania [50].

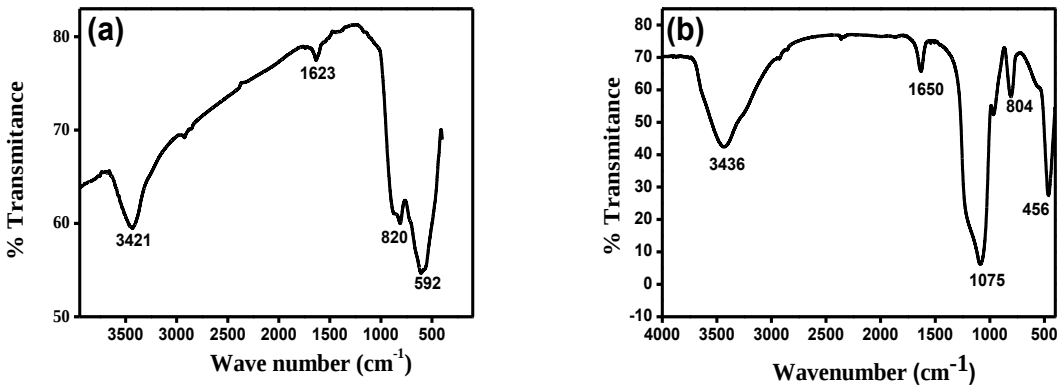


**Fig.5**. FT-IR spectra of (a) $TiO_2$ (b) $Ni_{0.10}$:$La_{0.05}$:$TiO_2$

### 3.1.5. Transmission Electron Microscope (TEM) and EDX.

TEM images were clearly displayed the morphology and particle size of neat $TiO_2$ and Nickel and lanthanum doped $TiO_2$. From the Fig. 6 we find that Nickel and lanthanum doped modified $TiO_2$ change the size of neat $TiO_2$ significantly, as shown in Fig. 6(a) and (b). The sizes of both modified and neat $TiO_2$ are mono disperse about 100–200 nm. Moreover, the crystal lattice line can be clearly found in the TEM images. The aggregations of both kinds of particles are caused by high surface energy; however, the agglomeration of the modified one is alleviated obviously compared with that of the neat [51].

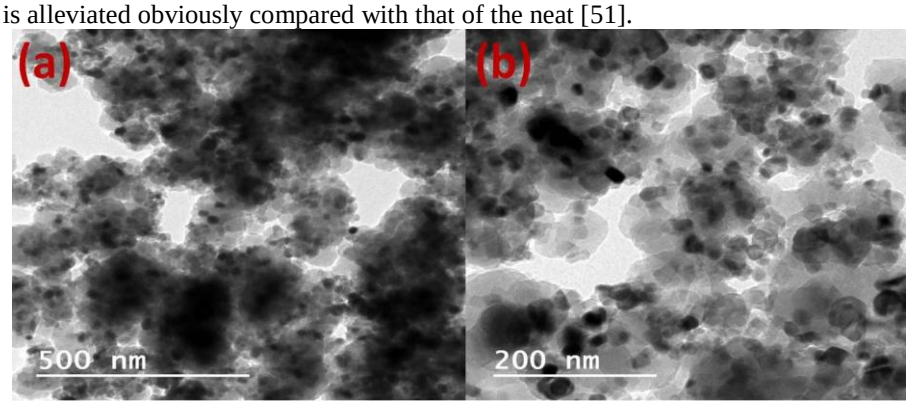


**Fig.6.** TEM image of the (A) $TiO_2$ (B) $Ni_{0.10}$:$La_{0.05}$:$TiO_2$

EDX Is an analytical technique used for the elemental analysis or chemical characterization of a sample. Compositional analysis of the nanomaterials can also be obtained by monitoring the X-rays produced by electron-specimen interaction. The formation and composition of crystalline $Ni_{0.10}$:$La_{0.05}$:$TiO_2$ nanocomposite was justified from EDX measurements. The compositional measurement of $Ni_{0.10}$:$La_{0.05}$:$TiO_2$ nanocomposite is showing in the Figure 7. The presence of La and Ni in the EDX is indicating that the metal ions of Ni and La have been impregnated in the Titania crystal. In the Figure the Cu is also observed this is due to the copper grid used in TEM analysis.

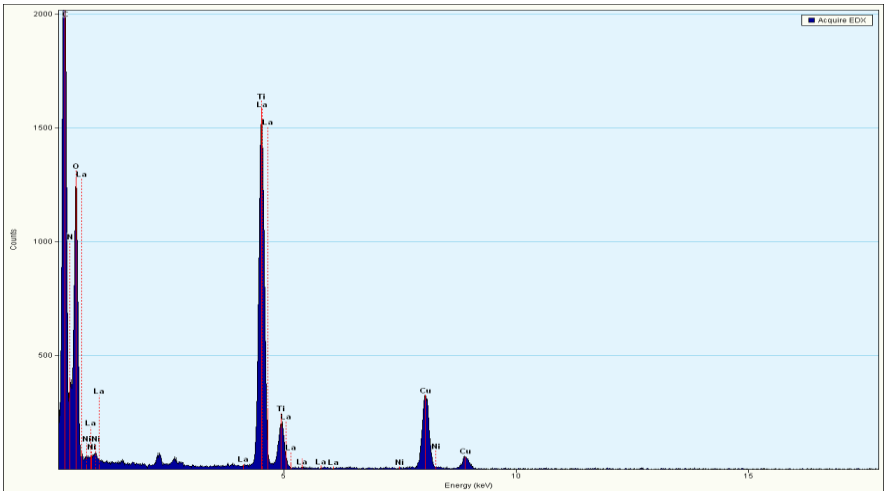


**Fig.7.** EDX image of $Ni_{0.10}$:$La_{0.05}$:$TiO_2$ nanocomposite

### 3.1.6. Scanning Electron Microscopy (SEM)

The morphology of the samples was investigated by scanning electron microscopy and it resumes the most interesting outcomes. Figure 8 (a) and 8 (b) clearly show that both the prepared samples are obtained in nanometric dimension. The impregnation of Nickel and lanthanum is indicating that the particle size reduce due the penetration of Nickel and lanthanum in the lattice of titanium dioxide [52].

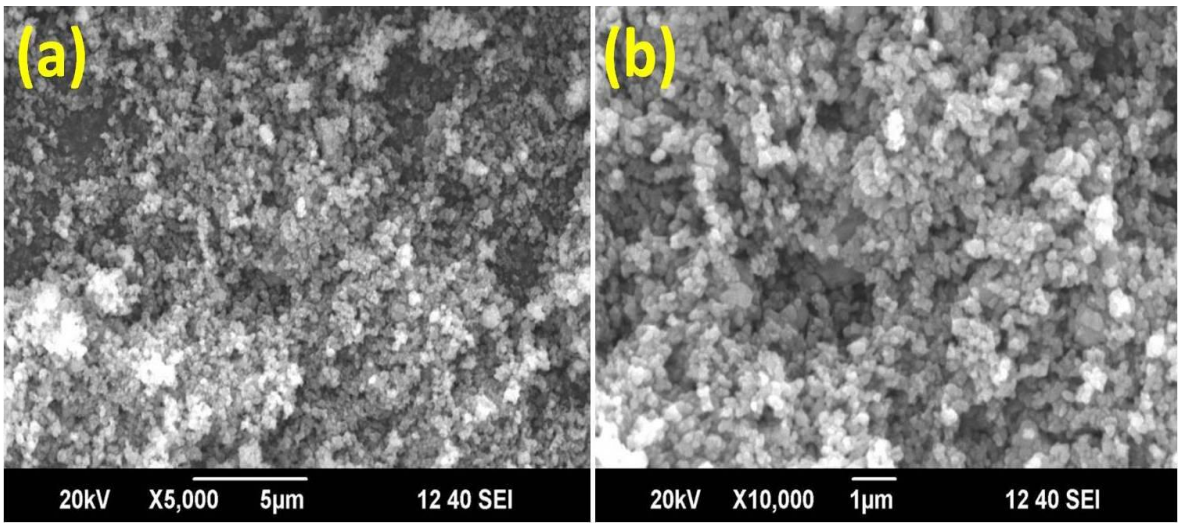


**Fig.8.** SEM image of the (A) $TiO_2$ (B) $Ni_{0.10}$:$La_{0.05}$:$TiO_2$

### 3.1.7. Surface Area Analysis (BET)

The specific surface area, pore volume and average pore size of the $TiO_2$ and $Ni_{0.10}$:$La_{0.05}$:$TiO_2$ photocatalyst were determine. Figure 9 showing the BET adsorption and desorption plots for the pure Titania and Ni, La impregnated Titania. Table 1 shown the physical properties of $TiO_2$ and $Ni_{0.10}$:$La_{0.05}$:$TiO_2$. The surface area of $TiO_2$ and $Ni_{0.10}$:$La_{0.05}$:$TiO_2$ was found 34.72 and 96.58 m2/g. The surface area of $Ni_{0.10}$:$La_{0.05}$:$TiO_2$ is increased rapidly with impregnation of Ni and La in pure Titania. The $TiO_2$ modified by Ni and La are fragmented to some extent during thermal treatment, leading to a marked increase of the *BET* surface areas and the average pore radius size and decreasing of the pore volume [53].

**Table 1:-** The specific surface area, pore volume and pore radius of the $TiO_2$ and $Ni_{0.10}$:$La_{0.05}$:$TiO_2$

| Sample | Surface area ($m^2$/g) | Pore volume ($cm^3$/g) | Pore radius (nm) |
|---|---|---|---|
| $TiO_2$ | 34. 72 | 11.132 | 1.21 |
| $Ni_{0.10}$:$La_{0.05}$:$TiO_2$ | 96.58 | 9.9124 | 1.64 |

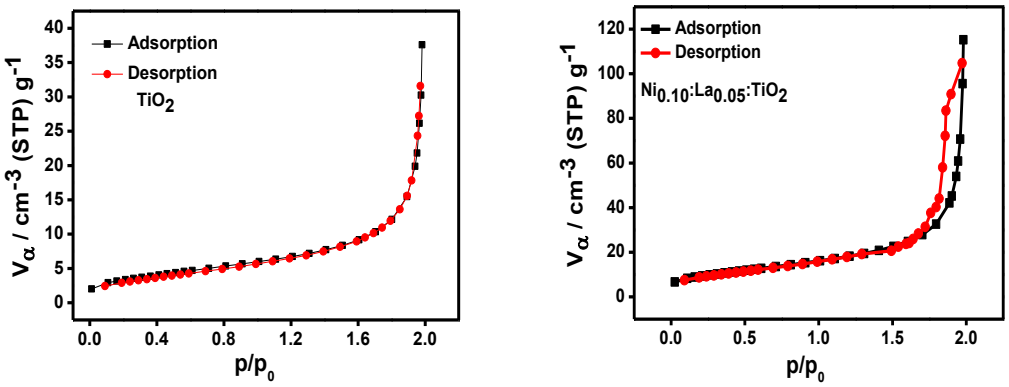


**Fig.9**. Adsorption and Desorption plots for Titania and Ni, La Impregnated Titania.

### 3.2. Adsorption study

A control experiment was first carried out under two conditions, vis (i) dye + UV (no $TiO_2$) (ii) $TiO_2$ + dye in dark without any irradiation (iii) $Ni_{0.10}$:$La_{0.05}$:$TiO_2$ + dye in dark without any irradiation (Figure 10). It can be seen that under dark conditions, after 20 min the amount of Methyl Green dye adsorbed becomes constant i.e. equilibrium adsorption is achieved. The reaction of Methyl Green in presence of $TiO_2$ and $Ni_{0.10}$:$La_{0.05}$:$TiO_2$ nanocomposites and UV irradiation is an example of heterogeneous catalysis. Rate laws in such reactions seldom follow proper law models and hence are inherently more difficult to formulate from the data. It has been widely accepted that heterogeneous catalytic reactions can be analyzed with the help of Langmuir Hinshelwood (LH) Model [54], with the following assumptions being satisfied:

(i). There are limited numbers of adsorption sites on the catalyst and its surface is homogeneous,
(ii). Only one molecule can be adsorbed on one site and monolayer formation occurs
(iii). The absorption reaction is reversible in nature, and
(iv). The adsorbed molecules do not react amongst themselves [55].

According to LH Model, following steps take place in the kinetics mechanism [56] (Adsorption of dye onto the catalyst surface). There are three steps of adsorption, Surface reaction, Desorption of products from the surface.

Step 1:- D (Dye) + C (catalyst) ⟷ D.C
Step 2:- D.C ⟷ E.C + Other products
Step 3:- E.C ⟷ E + C

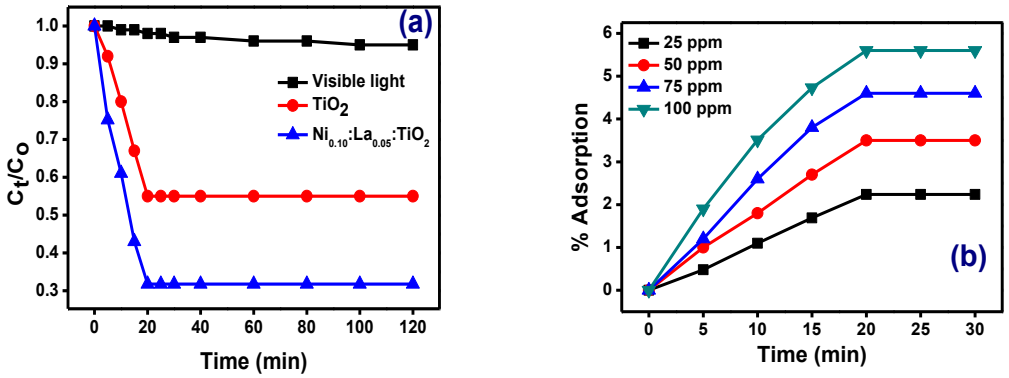


**Fig.10.** (a) change in concentration under dark with $TiO_2$, $Ni_{0.10}$:$La_{0.05}$:$TiO_2$ and in visible light (b) under dark with $Ni_{0.10}$:$La_{0.05}$:$TiO_2$ at different concentrations.

### 3.3. Photo-degradation of Dyes

The residual concentration of dye in the reaction mixture was measured spectrophotometrically. The results obtained for the degradation of Methyl Green is shown in Fig. 11-15.

**3.3.1. Effect of concentration of dye**

Effect of dye concentration keeping the catalyst loading concentration constant at 800 g/liter of the dye solution, the effect of varying concentration of the dye was studied on its rate of degradation (from 25 ppm to 100 ppm ) as given in Fig. 11. In presence of Titania the photodegradation of Methyl green dye was found 18% and 3% at 25 and 100 ppm concentration of dye solution. But in presence of $Ni_{0.10}$:$La_{0.05}$:$TiO_2$ the photodegradation was found 98.6 % and 56% at 25 ppm and 100ppm concentration of dye. With increasing concentration of Methyl Green the rate of degradation was found to decrease. This is because as the number of dye molecules increase, the amount of light (quantum of photons) penetrating the dye solution to reach the catalyst surface is reduced owing to the hindrance in the path of light. Thereby the formation of the reactive hydroxyl and superoxide radicals is also simultaneously reduced. Thus there should be an optimum value maintained for the catalyst and the dye concentration, wherein maximum efficiency of degradation can be achieved [34-39, 57].

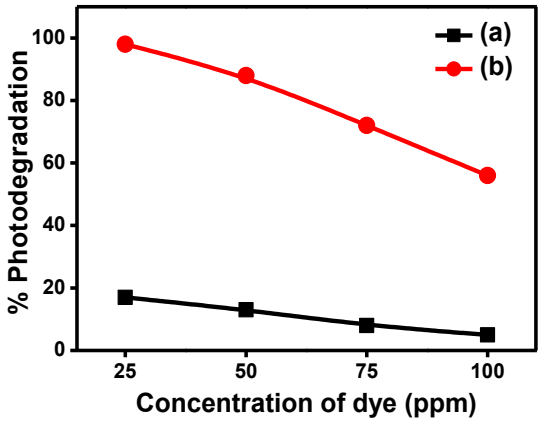


**Fig.11.** Effect of concentration on photodegradation of Methyl Green with (a) $TiO_2$ (b) $Ni_{0.10}$:$La_{0.05}$:$TiO_2$.

**3.3.2. Effect of irradiation Time on photodegradation**

The effect of irradiation time on the photodegradation of Methyl Green has been studied in presence of $Ni_{0.10}$:$La_{0.05}$:$TiO_2$. The photodegradation of Methyl Green was increased with increase irradiation time. The photodegradation was found maximum in 50 min irradiation of visible light. Figure 12 shows the effect of irradiation time on photocatalytic degradation of Methyl Green. This is because of the interaction of dye molecule with the surface of photocatalyst. The time of irradiation increase, the interaction of methyl green dye molecule increased with the surface of photocatalyst. Therefore the photodegradation efficiency of photocatalyst was increased [34, 36, 58].

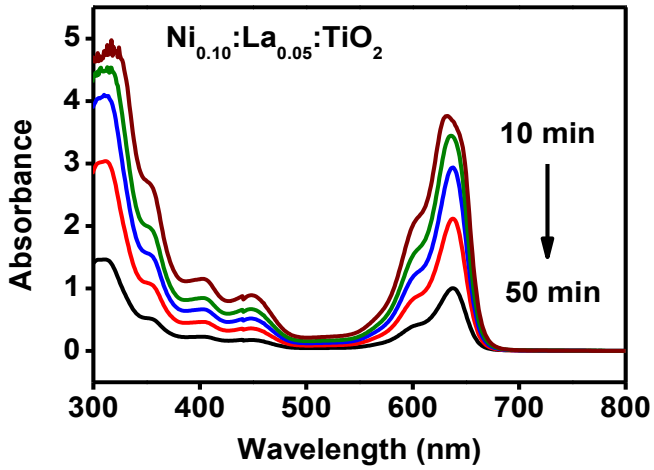


**Fig.12**. Effect of irradiation time on photocatalytic degradation of Methyl Green with $Ni_{0.10}$:$La_{0.05}$:$TiO_2$.

**3.3.3. Effect of pH of solution**

The photodegradation reaction was also carried out under varying pH from 4 to 9, by adjusting with $H_2SO_4$ and NaOH, with photocatalyst kept at constant amounts of 800 mg/L in the dye solutions (Figure 13). The maximum photodegradation of Methyl Green dye was found 17% and 88% in presence of $TiO_2$ and

$Ni_{0.10}$:$La_{0.05}$:$TiO_2$ at neutral medium or 7 pH of solution. The reaction of photodegradation was found low rates at acidic and basic ranges of pH. While at pH 7 or neutral medium, the photodegradation was found maximum. This implies that neutral conditions are favourable towards the formation of the reactive intermediates that is hydroxyl radicals is significantly enhanced, which further help in enhancing the reaction rate. There is another region that the Methyl Green is the dicationic dye which has 2+ charges. The surface of photocatalyst has slightly negative which can interact to positive dye molecule easily in the solution. On the other hand in highly acidic medium conditions for the formation of reactive intermediates is relatively less favourable and hence less spontaneous [40-42, 58].

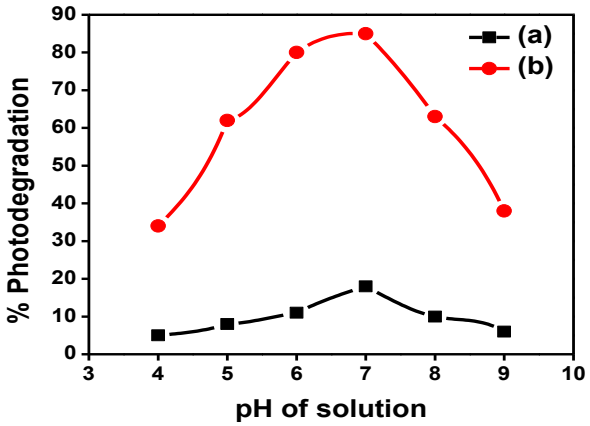


**Fig.13.** Effect of pH on photodegradation of Methyl Green with (a) $TiO_2$ and (b) $Ni_{0.10}$:$La_{0.05}$:$TiO_2$.

**3.3.4. Effect of photocatalyst amount**

The effect of photocatalyst amount has been studied by applying the different amount (100 ppm to 1600 ppm) of the photocatalyst. The photodegradation rate was found to increase by increasing the amount of photocatalyst but still a limited amount of photocatalyst, after certain amount of photocatalyst, the photodegradation is decreasing. The maximum photodegradation was found 99.2 and 21 % at 800mg/L amount of photocatalyst in presence of $Ni_{0.10}$:$La_{0.05}$:$TiO_2$ nanocomposite and $TiO_2$ respectively.

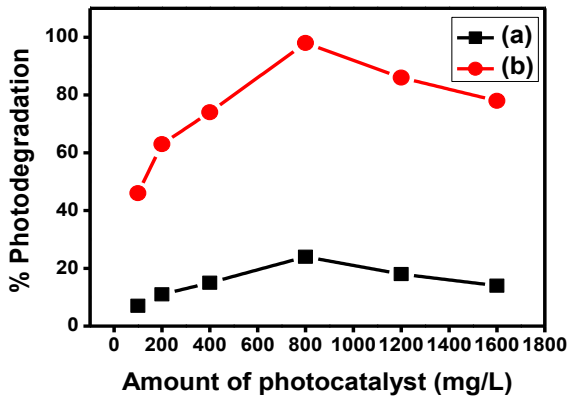


**Fig.14.** Effect of amount of photocatalyst on photodegradation of Methyl Green with (a) $TiO_2$ (b) $Ni_{0.10}$:$La_{0.05}$:$TiO_2$.

It is clear from the results shown in Figure14, the photodegradation increased rapidly with increase of amount from 100 mg/L to 800mg/L of $Ni_{0.10}$:$La_{0.05}$:$TiO_2$. We were found that when increase the amount of photocatalyst from 800mg/L to 1600mg/L, the photodegradation of dye rapidly decreased. This is due to the photocatalyst and dye molecule is properly interacting to each other till the 800mg/L amount of photocatalyst. After 800mg/L amount of photocatalyst, the turbidity increased in the solution due to photocatalyst molecules. The light (photon) is not striking on the surface of molecule. Therefore, the interaction between dye molecule and photocatalyst is decreased in some amount. The introduction of $Ni^{2+}$ and $La^{3+}$ ions in $TiO_2$, the surface area of photocatalyst was increased which increased the photocatalytic activity of Titania [43, 59].

**3.3.5. Effect of photocatalyst**

It is clear from the results shown in Fig.11-14 that $Ni_{0.10}$:$La_{0.05}$:$TiO_2$ is effective photo-catalyst for the degradation of Methyl Green (MG) dye than pure $TiO_2$. However $Ni_{0.10}$:$La_{0.05}$:$TiO_2$ seems to be more effective as photocatalyst for the degradation of Methyl Green (MG). The prominent degradation of Methyl Green was found in 50 min study in the presence of $Ni_{0.10}$:$La_{0.05}$:$TiO_2$ in comparison to the prepared $TiO_2$ [42, 59].

**3.4. Lowering of electron-hole recombination**

Photoluminescence spectra have been used to examine the mobility of the charge carriers to the surface as well as the recombination process involved by the electron-hole pairs in semiconductor particles. PL emission results from the radiative recombination of excited electrons and holes. In other words, it is a critical necessity of a good photocatalyst to have minimum electron-hole recombination. To study the recombination of charge carriers, PL studies of synthesized materials have been undertaken. PL emission intensity is directly related to recombination of excited electrons and holes. Fig. 15 shows the photoluminescence spectra of synthesized photocatalysts. In the PL spectra the intensity of $TiO_2$ is higher than $Ni_{0.10}$:$La_{0.05}$:$TiO_2$ indicating rate of recombination of $e^-$- $h^+$ is higher in $TiO_2$ than that of $Ni_{0.10}$:$La_{0.05}$:$TiO_2$ .The weak PL intensity of $Ni_{0.10}$:$La_{0.05}$:$TiO_2$ may arise due to the impregnation of Ni in Titania lattice, which for sub band level in band gap region of $TiO_2$. This delays the electrons- holes recombination process and hence utilized in the redox, reaction leading to improved photocatalytic activity [60].

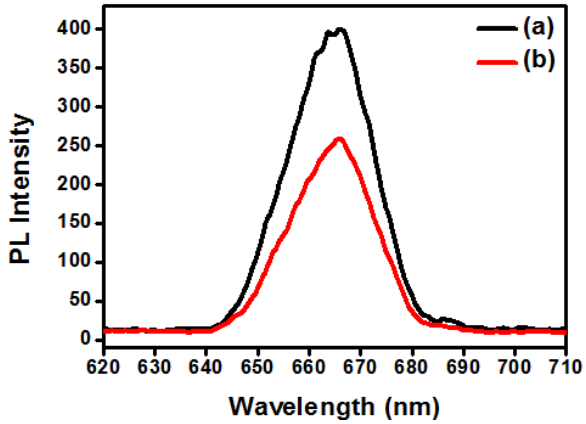


**Fig.15**. Photolumiscence Spectra of (a) $TiO_2$ and (b) $Ni_{0.10}$:$La_{0.05}$:$TiO_2$

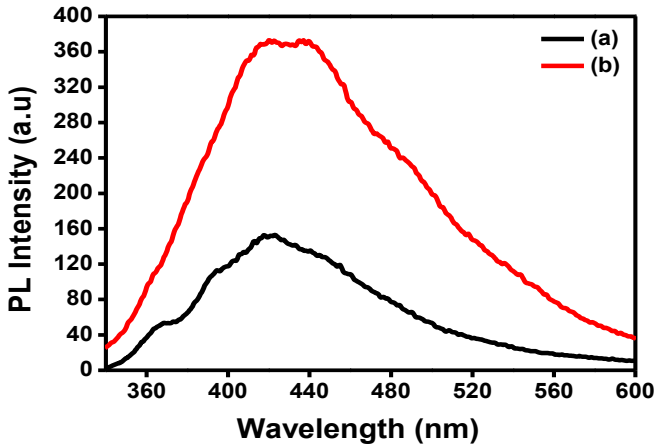


**Fig.16.** PL spectra of (a) $TiO_2$ and (b) $Ni_{0.10}$:$La_{0.05}$:$TiO_2$ photocatalyst with terephthalic acid (0.001M) in visible light

As hydroxyl radical performs the key role for the decomposition of the organic pollutants, it is necessary to investigate the amount of hydroxyl radicals produced by each photocatalyst. In this study terephthalic acid (TA) has been used as a probe reagent to evaluate $^{\bullet}OH$ radical present in the photoreaction pathway. Fig. 16 shows the PL spectra of $TiO_2$ and $Ni_{0.10}$:$La_{0.05}$:$TiO_2$ recorded Methyl Green solution in presence of $10^{-3}$M Terephthalic solution. OH radical attack Terephthalic Acid, forming 2- hydroxyl terephthalic acid (TAOH) which gives a fluorescence signal at 426 nm. The fluorescent intensity is linearly related to the number of hydroxyl radicals formed by the photocatalysts. Higher the generation of hydroxyl radical, more will be yield of TAOH and hence more intense will be the fluorescence peak. The spectra show that the intensity of

peak indicating in presence of $Ni_{0.10}$:$La_{0.05}$:$TiO_2$ higher generation of more number of hydroxyl radicals compared to $TiO_2$ [61].

### 3.5. Kinetic study

The data plotted in Fig. 17 were used for the calculation of the apparent kinetic constants for different reaction conditions. The rate of degradation of organic compounds in wastewaters can be described by a pseudo-first order Langmuir–Hinshelwood kinetic model [62-63]:

$$r = -\frac{dC}{dt} = \frac{CK\,K_r}{1+KC} \qquad (6)$$

where r stands for the rate of degradation, K represents the equilibrium constant for the adsorption of MG on the catalyst surface, and kr denotes the kinetic constant for the degradation reaction at maximum surface coverage. On integrating Eq. (6), we obtain the irradiation time, t, for attaining a concentration $C_t$ of the MG:

$$t = \left(\frac{1}{Kk_r}\right)\ln\left(\frac{C_0}{C_t}\right) + \frac{C_0 - C_t}{k_r} \qquad (7)$$

where $C_o$ represents the initial concentration of MG. Therefore at low $C_o$, the second term in Eq. (7) becomes insignificant and hence can be neglected:

$$\ln\left(\frac{C_0}{C_t}\right) = k_r K t = k_{app} t \qquad (8)$$

With $k_{app}$ as the apparent rate constant for the photocatalytic degradation reaction. The almost perfect linearity of the $\ln(C_o/C_t)$ versus t plots for various initial MG concentrations, Fig. 17, proves the applicability of the Langmuir–Hinshelwood equation for the photocatalytic degradation of MG [64]. The apparent rate constant, kapp, decreases as the initial concentration of MG increases. At too high MG concentrations, a greater amount of dye molecules adsorb on the catalyst surface blocking the photocatalytically active sites on the catalyst, thus reducing the absorption of photons, their interaction with the active sites and therefore inhibiting the photocatalytic degradation process. In addition, increasing MG concentration leads to a larger fraction of the UV irradiation that is absorbed by the dye molecules in the water solution, instead of being absorbed by the catalytically active sites [64-66]. The effect of Temperature on rate constant has been studied. The rate constant was found 0.0050 and 0.0062 $min^{-1}$in presence of Titania at 30 $^oC$ and 40 $^oC$ temperature of reaction. The rate constant is slightly increased with increase of temperature. The rate constant was found 0.0072 and 0.0102 $min^{-1}$ in presence of $Ni_{0.10}$:$La_{0.05}$:$TiO_2$ nanocomposite at 30 $^oC$ and 40 $^oC$ temperature of reaction. The rate constant of the photocatalysis is increasing with increase of temperature. This is due to the rate of reaction increased with increasing the temperature. The kinetic energy of dye molecule is increase with increase of temperature, which causes the interaction of dye molecule with photocatalyst. Hence the rate of reaction and rate constant are increased with increasing the temperature of reaction.

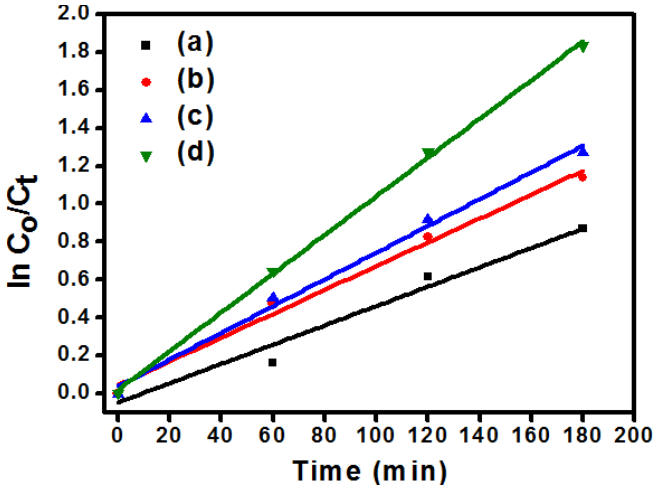


**Fig.17**.The straight line relationship between the ln ($C_o$/ $C_t$) and irradiation time indicates photodegradation rate of Methyl Green (50 ppm) can be approximated by a pseudo first order reaction (a) $TiO_2$ at 30$^oC$ (b) $TiO_2$ at 40$^oC$ (c) $Ni_{0.10}$:$La_{0.05}$:$TiO_2$ at 30$^oC$ (d) $Ni_{0.10}$:$La_{0.05}$:$TiO_2$ at 40$^oC$.

## IV. Conclusion

Prepared nanocomposites of $Ni_{0.10}$:$La_{0.05}$:$TiO_2$ were characterized by X-Ray Diffractometer, SEM, TEM, UV- Vis, FT-IR, Band gap energy and BET. The $TiO_2$ and $Ni_{0.10}$:$La_{0.05}$:$TiO_2$ were used as photocatalyst for the degradation of Methyl Green. The particle size was estimated by the Scherrer's and found 76 and 34 nm for $TiO_2$ and $Ni_{0.10}$:$La_{0.05}$:$TiO_2$ respectively. The XRD pattern confirmed the presence of anatase and rutile phase in the catalyst. The particle morphology of the photocatalysts was found in nanodiamension. The surface area of

$TiO_2$ and $Ni_{0.10}$:$La_{0.05}$:$TiO_2$ were found 34.72 and 96.58 $m^2$/g. The band gap energy of $TiO_2$ and $Ni_{0.10}$:$La_{0.05}$:$TiO_2$ were 3.2 and 3.0 eV. The photocatalytic degradation behaviour of photocatalysts was investigated by considering different parameters such as effect of concentration, effect of amount of photocatalyst, effect of pH, effect of temperature, adsorption and kinetics. The photodegradation of Methyl Green has been found 90-98 % at 7 pH, 25 ppm concentration of dye, 800 mg/L amount of photocatalyst and 50 min illumination of visible light in presence of $Ni_{0.10}$:$La_{0.05}$:$TiO_2$ while 10-18 % in presence of neat $TiO_2$ . The photodegradation was following the first order kinetics.

## Acknowledgement

We thanks for financial assistance to UGC, Government of India is acknowledged. The authors also acknowledge the support provided by the Babasaheb Bhimrao Ambedkar University, Lucknow, India

## References

[1]. Duxbury, D. F. The photochemistry and photophysics of triphenylmethane dyes in solid and liquid media. Chem. Rev. 93 (1), 1993, 381-433.
[2]. Inoue, T.; Kikuchi, K.; Hirose, K.; Iiono, M.; Nagano, T. Small molecule-based laser inactivation of inositol 1, 4, 5-triphosphate receptor. Chem. Biol. 8 (1), 2001, 9-15.
[3]. Green, F. J. The Sigma-Aldrih Handbook of Stains, Dyes, and Indicators; Aldrich Chemical: Milwaukee, WI, 1990.
[4]. Geethakrishnan, T.; Palanisamy, P. K. Degenerate four-wave mixing experiments in methyl green dye-doped gelatin film. Optik 117 (6), 2006, 282-286.
[5]. Melnick, J.; Pickering, M. The mechanism of the drug induced partial displacement of methyl green from DNA. Biochem. Int. 16 (1), 1988, 69-75.
[6]. Bonnett, R.; Martinez, G. Photobleaching of sensitisers used in photodynamic therapy. Tetrahedron, 57 (47), 2001,9513-9547.
[7]. Cho, B. P.; Yang, T.; Blankenship, L. R.; Moody, J. D.; Churchwell, M.; Bebland, F. A.; Culp, S. J. Synthesis and characterization of N-de-methylated metabolites of malachite green and leucomalachite green. Chem. Res. Toxicol. 16 (3), 2003, 285-294.
[8]. M. Vautier, C. Guillard, J.M. Herrmann, Photocatalytic degradation of dyes in water: Case study of Indigo and of Indigo Carmine, J. Catal. 201, 2001, 46–59.
[9]. S. Yang, X. Yang, X. Shao, R. Niu, L. Wang, Activated carbon catalyzed persulfate oxidation of Azo dye acid Green 7 at ambient temperature, J. Haz. Mater. 186, 2011, 659–666.
[10]. C.C. Chen and C. Shinlu, mechanistic studies of the Photocatalytic degradation of Methyl green: an investigation of Products of the decomposition Processes, environ. Sci. Technol. 41, 2007, 4389-4396
[11]. A. Jain, A. Ashma, K. Marazban, Expedient degradation of dye methyl green by enhanced photo–fenton process: a green chemical approach, J. Appl. Chem. 2, 2014, 13–25.
[12]. Nezamzadeh-Ejhieh, E. Shahriari, Photocatalytic decolorization of methyl green using Fe(II)-ophenanthroline as supported onto zeolite Y, J. Ind. Eng. Chem. 20, 2014, 2719–2726.
[13]. M. Nag, P.C. Chen, S. Kumar, Hydrothermal crystallization of titania on silver nucleation sites for the synthesis of visible light nano-photocatalysts—Enhanced photoactivity using Rhodamine 6G, Applied Catalysis A: General, 433–434, 2012, 75-80
[14]. A. Kumar, G. Pandey, Photocatalytic degradation of Eriochrome Black-T by the Ni:TiO2 nanocomposites, Desalination and Water Treatment, 71, 2017, 406–419, doi: 10.5004/dwt.2017.20541
[15]. P.V. Kamat, K. Vinodgopal, D.E. Wynkoop, Environmental photochemistry on semiconductor surfaces: photosensitized degradation of a textile azo dye, acid Green 7, on TiO2 particles using visible light. Environ. Sci. Technol, 30, 1996, 1660–1666.
[16]. R. Byberg, J. Cobb, L.D. Martin, R.W. Thompson, T.A. Camesano, O. Zahraa, M.N. Pons, Comparison of photocatalytic degradation of dyes in relation to their structure, Environ. Sci. Pollut. Res. 20, 2013, 3570–3581.
[17]. R. Montan, E. Rivero, Influence of activated carbon upon the photocatalytic degradation of methylene blue under UV–vis irradiation, Environ. Sci. Pollut. Res. 22, 2015, 784–791.
[18]. S. Choudhury, M. Dey and A. Choudhury, Defect generation, d-d transition, and band gap reduction in Cu-doped TiO2 nanoparticles, International Nano Letters, 3, 2013, 25
[19]. G. A. Epling, Chitsan Lin, ,Investigation of retardation effects on the titanium dioxide photodegradation system Chemosphere, 46, 2002, 937-944
[20]. M. Toyoda, T. Yano, B. Tryba, S. Mozia, T. Tsumura, and M. Inagaki, , Preparation of carbon-coated Magneli phases $Ti_nO_{2n-1}$ and their photocatalytic activity under visible light, Applied Catalysis B: Environmental, 88, 2009, 160-164.
[21]. X. Chen, & S. S. Mao, Titanium dioxide nanomaterials: Synthesis, properties, modifications, and applications. Chemical Reviews, 107, 2007, 2891–2959.
[22]. O. Jongprateep, R. Puranasamriddhi, J. Palomas Nanoparticulate titanium dioxide synthesized by sol-gel and solution combustion techniques, Ceramics International, 41, 2015, S169-S173
[23]. H. Lee, Y.K. Park, S.J. Kim, B.H. Kim, S.C. Jung, titanium dioxide modification with Nickel oxide nanoparticles for photocatalysis, Journal of Industrial and Engineering Chemistry, 32, 2015, 259-263
[24]. A. Kumar and G. Pandey, Photocatalytic Activity of Co:TiO2 Nanocomposites and their Application in Photodegradation of Acetic Acid, Chemical Science Transactions 6(3), 2017, 385-392, DOI:10.7598/cst2017.1378
[25]. H. Jia, Z. Zheng, H. Zhao, L. Zhang, and Z. Zou, aqueous sol–gel synthesis and growth mechanism of single crystalline $TiO_2$ nanorods with high photocatalytic activity, Materials Research Bulletin, 44, 2009, 1312-1316

[26]. A. Kumar, G. Pandey. Synthesis of La:Co:$TiO_2$ Nanocomposite and Photocatalytic Degradation of Tartaric Acid in Water at Various Parameters. American Journal of Nano Research and Applications. 5, (4), 2017, 40-48. doi: 10.11648/j.nano.20170504.11

[27]. N. M. Makwana, C. J. Tighe, R.I. Gruar, P. F. McMillan, Pilot plant scale continuous hydrothemal synthesis of nano-titania; effect of size on photocatalytic activity, Materials Science in Semiconductor Processing, 42, 2016, 131-137

[28]. A. Kumar, G. Hitkari, M. Gautam, S. Singh, G. Pandey, Synthesis, Characterization and Application of Cu-$TiO_2$ Nanaocomposites in Photodegradation of Methyl Red (MR), Int. Adv. Res. J. in Sci., Eng. and Tech., 2, 2015, 50-55, DOI 10.17148/ IARJSET.2015.21208

[29]. A. M. Ng, P.C. Chen, S. kumar, Hydrothermal crystallization of titania on silver nucleation sites for the synthesis of visible light nano-photocatalysts—Enhanced photoactivity using Rhodamine 6G, Applied Catalysis A: General, 433–434, 2012, 75-80.

[30]. M. Hema, A.Y. Arasi, P. Tamilselvi, R. Anbarasan,, Titania nanoparticles synthesized by sol–gel technique, Chem. Sci. Trans. 2, 2013, 239–245.

[31]. A. Kumar, G. Hitkari, M. Gautam, S. Singh, G. Pandey, Synthesis of Ni-TiO2 Nanocomposites and Photocatalytic Degradation of Oxalic Acid in Waste Water, Int. J. of Inn. Res. in Sci., Eng. and Tech. 4, 2015, 12721-12731, DOI:10.15680/IJIRSET.2015.0412097

[32]. B. D. Cullity, S. R. Stock, , Elements of X-Ray Diffraction, Third Edition, and New Jersey: Prentice-Hall, Inc., 2001.

[33]. A. Pal, R. Kaur, I. S. Grover, Superior adsorption and photodegradation of Eriochrome black-T dye by $Fe^{3+}$ and $Pt^{4+}$ impregnated $TiO_2$ nanostructures of different shapes , J. of Ind. and Eng. Chem., 33, 2016, 178-184

[34]. H. Lachheb, E. Puzenat, A. Houas, M. Ksibi, E. Elaloui, C. Guillard, J.M. Herrmann, Photocatalytic degradation of various types of dyes (Alizarin S, Crocein Green G, Methyl Red, Congo Red, Methylene Blue) in water by UV-irradiated titania, Appl. Catal. B: Environ. 39, 2002, 75–90.

[35]. Pare, P. Singh and S.B. Jonnalgadda, Degradation and mineralization of Victoria Blue B dye in a slurry photo reactor using advanced oxidation process, Journal of Scientific & Industrial Research, 68, 2009, 724-729.

[36]. W. Baran , A. Makowski, W. Wardas, The influence of FeCl3 on the photocatalytic degradation of dissolved azo dyes in aqueous TiO2 suspensions, Chemosphere 53,2003, 87–95.

[37]. A. Gnanaprakasam, V.M. Sivakumar, P.L. Sivayogavalli, M. Thirumarimurugan Characterization of TiO2 and ZnO nanoparticles and their applications in photocatalytic degradation of azodyes , Ecotoxicology and Environmental Safety, 121, 2015, 121-125

[38]. S. Kaur, V. Singh, Visible light induced sonophotocatalytic degradation of Reactive Red dye 198 using dye sensitized $TiO_2$ Ultrasonics Sonochemistry, 14, 2007, 531-537

[39]. G.A. Epling, C. Lin, Photoassisted bleaching of dyes utilizing TiO2 and visible light, Chemosphere 46, 2002, 561–570.

[40]. A. Kumar, G. Pandey, Photodegradation of Methyl Green in Aqueous Solution by the Visible Light Active Co:La:$TiO_2$ Nanocomposite. Chem Sci J 8, 2017,164. doi: 10.4172/2150-3494.1000164

[41]. H. B, Hadjltaief, M. B. Zinaa, M. E. Galvezb, P. D. Costa, Photocatalytic degradation of methyl green dye in aqueous solution over natural clay-supported ZnO–TiO2 catalysts Journal of Photochemistry and Photobiology A: Chemistry 315, 2016, 25–33

[42]. M. Vautier, C. Guillard, J.M. Herrmann, Photocatalytic degradation of dyes in water: Case study of Indigo and of Indigo Carmine, J. Catal. 201, 2001, 46–59.

[43]. M.M. Ba-Abbad, A.A.H. Kadhum, A.B. Mohamad, M.S. Takriff, K. Sopian, Synthesis and catalytic activity of $TiO_2$ nanoparticles for photochemical oxidation of concentrated chlorophenols under direct solar radiation, Int. J. Electrochem. Sci 7, 2012, 4871–4888.

[44]. S. Kumari, Y.S. Chaudhary, S.A. Agnihotry, C. Tripathi, A. Verma., D. Chauhan., R. Shrivastav, S. Dass., and V.R. Satsangi., A photoelectrochemical study of nano structured Cd-doped titanium oxide, Int. J. of Hydrogen Energy, 32, 2007, 1299-1302.

[45]. J. Peral, X. Domenech, D.F. Ollis, Heterogeneous photocatalysis for purification, decontamination and deodorization of air, J. Chem. Technol. Biotechnol. 70, 1997, 117–140.

[46]. J. Zhu, Z. Deng, F. Chen, J. Zhang, H. Chen, M. Anpo, J. Huang, L. Zhang, Hydrothermal impregnation method for preparation of $Cr^{3+}$-TiO2 photocatalysts with concentration gradient distribution of $Cr^{3+}$, Appl. Catal. B: Environ. 62 , 2006, 329–335.

[47]. J.C. Colmenares, M.A. Aramendia, A. Marinas, J.M. Marinas, F.J. Urbano, Synthesis, characterization and photocatalytic activity of different metal-doped titania systems, Appl. Catal. A: Gen. 306, 2006, 120–127.

[48]. Y. Ao, F.J.D. Xu, X. Shen, C. Yuan, Low temperature preparation of anatase $TiO_2$- coated activated carbon, Colloids Surf. A Physicochem. Eng. Aspects 312, 2008, 125–130.

[49]. K. M. Reddy, S. V. Manorama, A. R. Reddy, Bandgap studies on anatase titanium dioxide nanoparticles, Materials, Chemistry and Physics 78, 2002, 239–245.

[50]. X. Chen, S. S. Mao, Titanium dioxide nanomaterials: Synthesis, properties, modifications, and applications. Chem. Rev. 107, 2007, 2891−2959.

[51]. A. Sobczynski, A. Dobosz, Water purification by photocatalysis on semiconductors. Pol. J. Environ. Stud. 10, 2001, 195-205.

[52]. G. Tian, K. Pan, H. Fu, L. Jing, W. Zhou, Enhanced photocatalytic activity of S-doped $TiO_2$−$ZrO_2$ nanoparticles under visible-light irradiation. J. Hazard. Mater. 166, 2009, 939−944.

[53]. X. Cheng, H. Liu, Q. Chen, J. Li, P. Wang, Construction of N, S codoped $TiO_2$ NCs decorated $TiO_2$ nano-tube array photoelectrode and its enhanced visible light photocatalytic mechanism. Electrochim. Acta, 103, 2013, 134−142.

[54]. H. Freundlich, Ueber die adsorption in loesungen, J. Phys. Chem. 57, 1907, 385–470.

[55]. Langmuir, The adsorption of gases on plane surfaces of glass, mica and platinum, J. Am. Chem. Soc.40, 1918, 1361–1403.

[56]. R.W. Matthews, Kinetics of photocatalytic oxidation of organic solutes over titanium dioxide, J. Catal. 111, 1988, 264–272.

[57]. Vulliet, J.M. Chovelon, C. Guillard, J.M. Herrmann, Factors influencing the photocatalytic degradation of sulfonylurea herbicides by TiO2 aqueous suspension, J. Photochem. Photobiol. A: Chem. 159, 2003, 71–79.

[58]. U.G. Akpan, B.H. Hameed, Parameters affecting the photocatalytic degradation of dyes using TiO2-based photocatalysts: A review, Journal of Hazardous Materials 170, 2009, 520–529
[59]. K. M. Reza, ASW Kurny, F. Gulshan, Parameters affecting the photocatalytic degradation of dyes using $TiO_2$: a review, Appl Water Sci , 7, 2017, 1569–1578
[60]. G. K. Pradhan, D. Padhi, and K. Parida, Fabrication of #-$Fe_2O_3$ Nanorod/RGO composite: A novel hybrid photocatalyst for phenol degradation, Appl. Mater. Interfaces 5, 2013, 9101–9110
[61]. T. Tachikawa, S. Tojo, M. Fujitsuka, T. Sekino, and T. Majima, Photoinduced Charge Separation in Titania Nanotubes, J. Phys. Chem. B, 110, 2006, 29
[62]. N. Guettaı, H.A. Amar, Photocatalytic oxidation of methyl Green in presence of titanium dioxide in aqueous suspension. Part II: Kinetics study, Desalination 185, 2005, 439–448.
[63]. N. Jallouli, K. Elghniji, O. Hentati, A. R. Ribeiro, A. M.T. Silva, M. K. sibi, UV and solar photodegradation of naproxen TiO2 catalyst effect, reaction kinetics, products identification and toxicity assessment, J. of Haz. Materials, 304, 5, 2016, 329-336
[64]. M.D. Murcia, N.O. Vershinin, N. Briantceva, M. Gomez, E. Gomez, E. Cascales, A.M. Hidalgo, Development of a kinetic model for the UV/$H_2O_2$ photodegradation of 2,4-dichlorophenoxiacetic acid, Chemical Engineering Journal, 266, 2015, 356-367
[65]. Z. Bensaadi, N.Y. Mezenner, M. Trari, F.Medjene, kinetic studies of β-blocker photodegradation on TiO2, J. of Envi. Chemi. Eng., 2, 2014, 1371-1377
[66]. Ahmad, R. Bano, S. G. Musharraf, M.A.Sheraz, S. Ahmed, H. Tahir, Q. U. Arfeen, M. S. Bhatti, Z. Shad, S. F. Hussain, photodegradation of norfloxacin in aqueous and organic solvents: A Kinetic study , Journal of Photochemistry and Photobiology A: Chemistry, 302, 2015, 1-10

IOSR Journal of Applied Chemistry (IOSR-JAC) is UGC approved Journal with Sl. No. 4031, Journal no. 44190.

Azad Kumar. "The photocatalytic degradation of Methyl Green in presence of Visible light with photoactive Ni0.10:La0.05:TiO2 nanocomposites." IOSR Journal of Applied Chemistry (IOSR-JAC), vol. 10, no. 9, 2017, pp. 31–44.